Int. J. Electrochem. Sci., 8 **(2013)** 4174 - 4182

International Journal of
ELECTROCHEMICAL
SCIENCE
www.electrochemsci.org

Controlled Fabrication of Iron Oxalate Hydrate Microstructures and Study of Their Electrochemical Properties

Huan Pang[1, 2, 3,*], *Shaomei Wang*[1], *Xuexue Li*[1], *Shanshan Zhao*[1], *Nannan Zhang*[1], *Jing Chen*[1], *Jiangshan Zhang*[1], *Honghe Zheng*[2,*] *and Sujuan Li*[1,*]

[1] College of Chemistry and Chemical Engineering, Anyang Normal University, Anyang, 455000, Henan, P. R. China.
[2] School of Energy, Soochow University, Suzhou, 215006, Jiangsu, P. R. China.
[3] State Key Laboratory of Coordination Chemistry, Nanjing University, Nanjing, 210093, Jiangsu, P. R. China.
[*]E-mail: huanpangchem@hotmail.com; hhzheng@suda.edu.cn; lisujuan1981@gmail.com

Received: 4 January 2013 / *Accepted:* 30 January 2013 / *Published:* 1 March 2013

Iron oxalate hydrate ($FeC_2O_4 \cdot 2H_2O$) microrods and microtubes are successfully synthesized under room temperature by a co-precipitation method. We also explore the formation mechanism of the microstructure. Interestingly, after electrochemical measurements of iron oxalate hydrate micromaterials, it indicates that $FeC_2O_4 \cdot 2H_2O$ microrods exhibit higher capacities close to 346 mA h/g after 100 cycles at 0.5 C (C=1 Li h^{-1} mol^{-1}) rate between 0 and 2 V.

Keywords: Iron oxalate hydrate; Microrods; Microtubes; Formation mechanism; Electrochemical measurement;

1. INTRODUCTION

Due to fast redox reactions, high specific surface areas and shortened diffusion paths in the solid phase, synthesized nanomaterials have raised an important and hot field in electrochemical energy storage. [1-5] One dimensional (1D) nanostructures, are perfect building blocks for functional nanodevices and represents the small dimension for efficient electron transport.[6, 7] Commonly, the electrical conductivity is one of the most important aspects of electrode materials, which can effectively enhance the utilization of active materials and mitigate the internal resistance of the battery. [8] Therefore the synthesis of one-dimensional nanostructures to be used in the field of nanoelectrode materials is highly desirable for materials scientists and researchers in materials engineering who study material properties.

During the past few decades, lithium (Li)-ion batteries have been widely used as energy sources of portable devices such as cell phones and laptops. Given the diverse applications of and demand for Li-ion batteries, safe and retainable electrode materials with high energy densities are needed to promote the large-scale application of these batteries as energy sources for hybrid electric or pure electric vehicles, or as stationary energy storage systems of intermittent substitutive energy sources (such as wind and solar) for intelligent grids. [9-13]

Currently, the most common approaches to metal oxalates are reverse-micellar route, solvothermal reaction sol–gel process, microwave-assisted solution approach and one step solid-state reaction. [14-23] As a simple method for fabricating nanomaterials at room temperature, one-step solid-state reaction has attracted considerable interest because complex process control, high reaction temperature or long synthesis time should not be required any more. [23-36]

Iron Oxalate, as one of most metal oxalates, has received considerable attention due to their broad and potential applications, and some progresses have been made. [37, 38] Herein, we have successfully synthesize iron oxalate hydrate ($FeC_2O_4 \cdot 2H_2O$) microrods and microtubes under room temperature by a co-precipitation method with glycol as the additive agent. More importantly, electrochemical measurements of iron oxalate hydrate micromaterials indicate that $FeC_2O_4 \cdot 2H_2O$ microrods exhibit higher capacities close to 346 mA h/g after 100 cycles at 0.5 C (C=1 Li h^{-1} mol^{-1}) rate between 0 and 2 V.

2. EXPERIMENTAL

2.1 Synthesis of $FeC_2O_4 \cdot 2H_2O$ microrods and microtubes

In a typical synthesis, I) $FeC_2O_4 \cdot 2H_2O$ microrods: 0.5 g $Fe(SO_4)_2$ and 0.4 g $Na_2C_2O_4$ respectively were added into 55 mL ethylene glycol (EG), and then the mixture was stirred for 24 hours at room temperature. After the reaction completed, the yellow $FeC_2O_4 \cdot 2H_2O$ precipitate obtained was collected by centrifuging, washed several times with distilled water and absolute ethanol, and finally dried in a vacuum oven at 25 ˚C for 12 h; II) $FeC_2O_4 \cdot 2H_2O$ microtubes: 5 mL EG and 50 mL water were firstly mixed together. Then 0.50 g $Fe(SO_4)_2$ and 0.40 g $Na_2C_2O_4$ respectively were added into the above solution. The mixture was stirred for 4 hours at room temperature. After the reaction completed, the yellow $FeC_2O_4 \cdot 2H_2O$ precipitate obtained was collected by centrifuging, washed several times with distilled water and absolute ethanol, and finally dried in a vacuum oven at 25 ˚C for 12 h.

2.2 Preparation of lithium ion battery electrodes

The anode materials (based $FeC_2O_4 \cdot 2H_2O$ mass) were fabricated by mixing $FeC_2O_4 \cdot 2H_2O$ micromaterials, acetylene black, and PVDF at a weight ratio of 70:20:10, respectively, using N-methylpyrrolidone (NMP) as a solvent. The resulting slurries were cast onto copper current collectors, and then dried at 120 ^oC under vacuum for 12 h. The electrode foils were pressed at a pressure of

8.27×10^6 Pa, and then cut into disks 13 mm in diameter. CR2016 coin-type cells were assembled in an argon-filled glove box (M-braun MB20G) by stacking a microporous polypropylene separator (Celgard 2400) containing a liquid electrolyte of $LiClO_4$ (1.0 M) in ethylene carbonate (EC)/dimethyl carbonate (DMC) (1:1, v/v) between the anode and the lithium metal foil.

2.3. Characterization

The morphology of the as-prepared samples was observed by a JEOL JSM-6701F field-emission scanning electron microscope (FE-SEM) at an acceleration voltage of 5.0 kV. The phase analyses of the samples were performed by X-ray diffraction (XRD) on a Ultima III with Cu Kα radiation (λ = 1.5418 Å). Transmission electron microscopy (TEM) images and HRTEM image were captured on the JEM-2100 instrument microscopy at an acceleration voltage of 200 kV. The batteries were tested on Land CT2001A.

3. RESULTS AND DISCUSSION

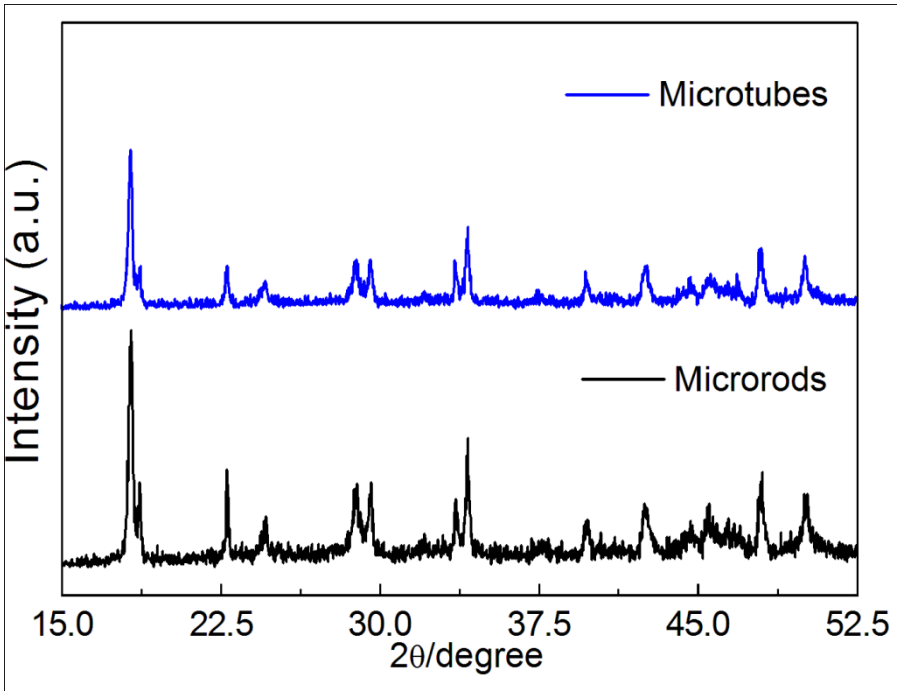

Figure 1. The XRD pattern of the as-prepared samples.

The XRD pattern of the as-prepared samples (Figure 1) demonstrates that all of the diffraction peaks can be readily indexed to pure ferrous oxalate dihydrate (JCPDS: 72-1305). No diffraction peaks from impurities were found in the sample.

Simply by controlling different conditions, $FeC_2O_4\cdot2H_2O$ microrods and microtubes have been obtained. The morphology of the as-synthesized $FeC_2O_4\cdot 2H_2O$ was examined with an FESEM. Figure 2a shows a typical low magnification image of the as-prepared $FeC_2O_4\cdot2H_2O$ sample, which clearly

demonstrates that the $FeC_2O_4 \cdot 2H_2O$ microrods are uniform with the width-550 nm and the length-1300 nm, and obtained on a large scale.

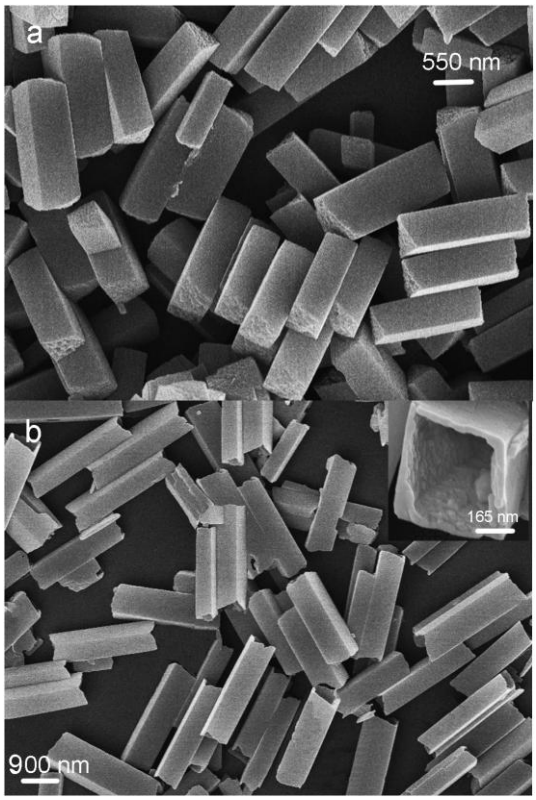

Figure 2. SEM images of as-prepared samples, (a) $FeC_2O_4 \cdot 2H_2O$ microrods; (b) $FeC_2O_4 \cdot 2H_2O$ microtubes.

In Figure 2b, the morphology of $FeC_2O_4 \cdot 2H_2O$ microtubes can be seen obviously. The length of a single microtube is the same as the microrod's. It is obviously that the diameter of a single microtube is 450-500 nm shown in inset of Figure 2b.

A transmission electron microscopy (TEM) images in Figure 3. In Figure 3a, the morphology of microrods is further confirmed. High-resolution TEM (HRTEM, Figure 3b) and selected area electron diffraction (SAED) in Figure 3c show that the crystallization of microrods is not good. In Figure 3d, the inner diameter of microtubes is not uniform and it has larger size for its two ends. From SAED of the end of microtubes, it also has not good crystallization. The wall of the microtube end is thinner than that of microtube middle.

We also explored the formation mechanism of the microstructure and have tried to find the reason effected morphologies of the product. The product was synthesized under different conditions, and their SEM images were shown in Figure 4. In Figure 4 c, d, the product is synthesized under the same condition as microtubes' except different stirred times. We find that the microrod is formed in pure EG solution. When used water-EG mixed solution, microtubes is easily obtained. The longer stirred time, the more microrods were etched. This phenomenon might be based the equation:

$$FeC_2O_4 \cdot 2H_2O + C_2O_4^{2-} == Fe[C_2O_4]_2^{2-} + 2H_2O$$

The $Fe[C_2O_4]_2^{2-}$ is water soluble, and the adding water makes this equation happen easily. A possible formation mechanism of the microstructure was also shown in Scheme 1, in which the morphology changed from microrods to microfilms. As adding water, microrods were etched into microtubes.

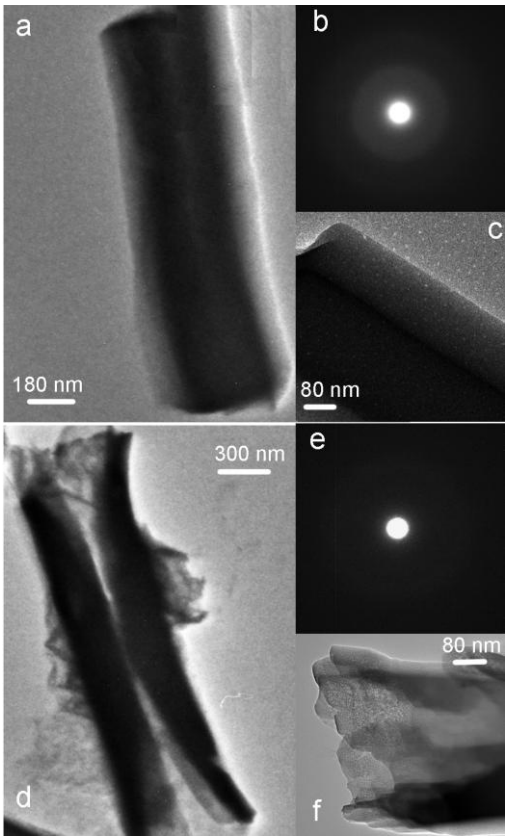

Figure 3. TEM images of as-prepared samples, (a, c) $FeC_2O_4 \cdot 2H_2O$ microrods; (d, f) $FeC_2O_4 \cdot 2H_2O$ microtubes; (b) selected area electron diffraction (SAED) of microrods; (e) SAED of microtubes.

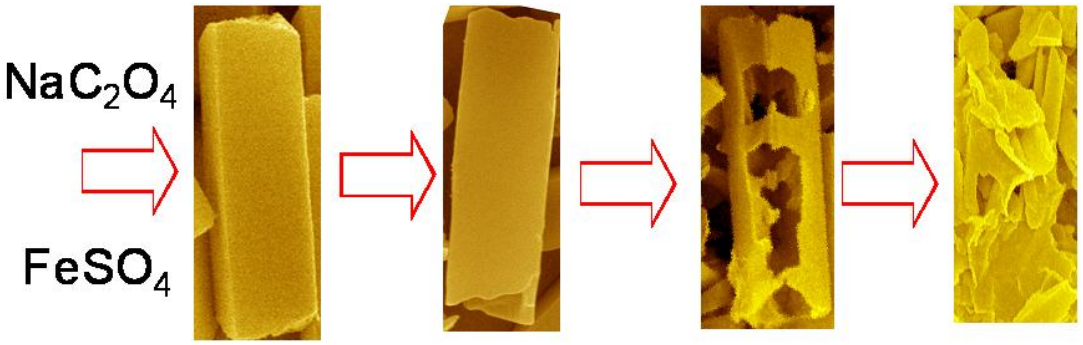

Scheme 1. Schematic illustration of the solid-hollow-slice formation process.

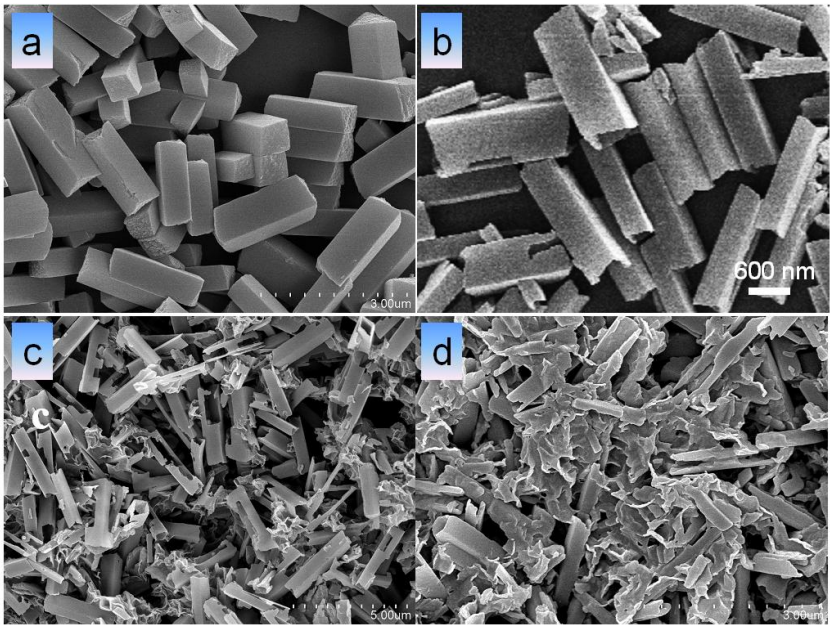

Figure 4. SEM images of as-prepared samples obtained under different conditions, (a) 0.5 g $Fe(SO_4)_2$ and 0.4 g $Na_2C_2O_4$ respectively were added into 55 mL ethylene glycol (EG), and then the mixture was stirred for 24 hours at room temperature; (b) 0.50 g $Fe(SO_4)_2$ and 0.40 g $Na_2C_2O_4$ were mixed with 5 mL EG and 50 mL water together for 4 hours at room temperature; (c) 0.50 g $Fe(SO_4)_2$ and 0.40 g $Na_2C_2O_4$ were mixed with 5 mL EG and 50 mL water together for 24 hours at room temperature; (d) 0.50 g $Fe(SO_4)_2$ and 0.40 g $Na_2C_2O_4$ were mixed with 5 mL EG and 50 mL water together for 48 hours at room temperature.

And then increasing the stirred time, the microtube is further to be etched in Figure 4c. After longer the stirred time, there are only microfilms or microslices left in Figure 4d. And at this time, the equation is balance. This phenomenon is also reported by many famous groups [39-41]

It is believed that different structures might lead to different electrochemical conditions for intercalated ion movement and electrolyte access. Figure 5 show discharge curves of the cells made from the as-prepared $FeC_2O_4{\cdot}2H_2O$ microrods, microtubes and commercial powders materials between 0.0–2.0 V at 0.5 C at room temperature. As can be seen from Figure 5a, the first cycle discharge capacities for the as-synthesized $FeC_2O_4{\cdot}2H_2O$ microrods, microtubes and commercial powders materials electrodes were 1340, 1730 and 833 mAh g^{-1}, respectively. All the electrodes show a certain capacity fade upon prolonged cycling in Figure 5b. However, $FeC_2O_4{\cdot}2H_2O$ microrods electrodes maintained fairly high Li-ion insertion/deinsertion capacity even after 100 cycles in Figure 5b. Compared with the other $FeC_2O_4{\cdot}2H_2O$ microtubes and commercial powders electrodes, we can see that $FeC_2O_4{\cdot}2H_2O$ microrods electrodes have good cycling performance which retain >346 mAh g^{-1} after 100 cycle. This result is better than the reference 37, and $FeC_2O_4{\cdot}2H_2O$ microrods electrodes show a longer cycle life.

Such superior rate capability of the $FeC_2O_4{\cdot}2H_2O$ microrods electrode should be attributed to many different reasons. The most important reasons must be associated with more easy paths for electrons, ions and electrolytes, such as: (1) the effective specific surface area for superstructures (Its BET surface area-$FeC_2O_4{\cdot}2H_2O$ microrods-49.1 $m^2 g^{-1}$; $FeC_2O_4{\cdot}2H_2O$ microtubes-32.0 $m^2 g^{-1}$); (2) the skeleton of $FeC_2O_4{\cdot}2H_2O$ microtubes electrodes is unstable for electrochemical charge-discharge

process, which caused short cycle life; (3) $FeC_2O_4 \cdot 2H_2O$ microrods may have novel surface-interface characters. Namely, these novel chemical-physical characters bring the novel surface-interface and diffusion paths, leading to in high electrochemical activities.

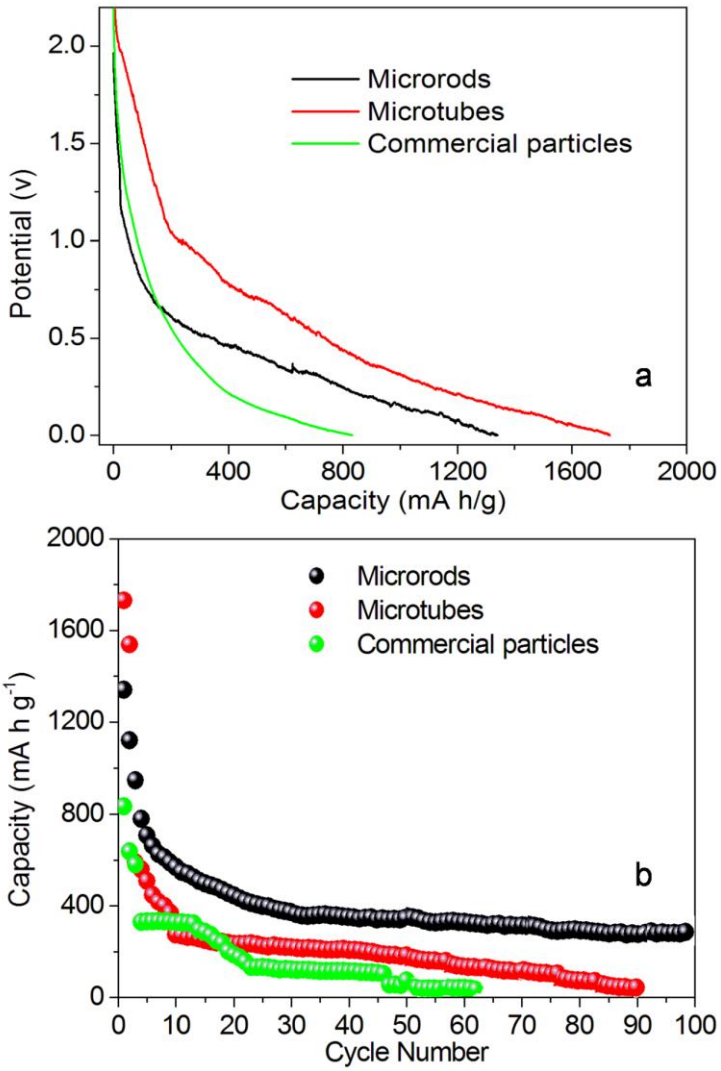

Figure 5. (a) Discharge curves of the cells made from the as-prepared materials between 0.0–2.0 V at 0.5 C at room temperature; (b) The long cyclic performances of the electrodes at 0.5 C.

4. CONCLUSIONS

In summary, $FeC_2O_4 \cdot 2H_2O$ microrods, microtubes have been successfully prepared via a simple co-precipitation approach with glycol as the additive agent. The morphologies and sizes of the as-prepared $FeC_2O_4 \cdot 2H_2O$ microstructures were well controlled by varying the reaction parameters. The $FeC_2O_4 \cdot 2H_2O$ microrods are favorable for increasing the discharge capacity and improving the electrode kinetics. $FeC_2O_4 \cdot 2H_2O$ microrods exhibited a high discharge capacity of 346 mAh g^{-1} (at 0.5

C) after 100 cycles. The present results suggests that $FeC_2O_4 \cdot 2H_2O$ microrods are promising anode materials in lithium ion batteries.

ACKNOWLEDGEMENTS
This work is supported by the National Natural Science Foundation of China (21201010, 21073129, 21071006 and 51272168). Henan Province of Science & Technology Foundation (122102210253) and the project of Science & Technology of Anyang city. China Postdoctoral Science Foundation (2012M521115).

References

1. Y. S. Jang, J. H. Kim, S. H. Choi, K. M. Yang and Y. C. Kang, *Int. J. Electrochem. Sci.* 7 (2012) 12531-12544.
2. N. Zhou, E. Uchaker, Y. Y. Liu, S. Q. Liu, Y. N. Liu and G. Z. Cao, *Int. J. Electrochem. Sci.* 7 (2012) 12633-12645.
3. H. Xu, B. Cheng, E. Xu, L. Xu, J. Yang and Y. Qian, *Int. J. Electrochem. Sci.* 7 (2012) 11917-11929.
4. H. Pang**,** J. Deng, B. Yan, Y. Ma, G. Li, Y. Ai, J. Chen, J. Zhang, H. Zheng and J. Du, *Int. J. Electrochem. Sci.* 7 (2012) 10735-10747.
5. H. Pang, Z. Yan, W. Wang, Y. Wei, X. Li, J. Li, J. Chen, J. Zhang and H. Zheng, *Int. J. Electrochem. Sci.* 7 (2012) 12340-12353.
6. C. Z. Wu, J. Dai, X. D. Zhang, J. L. Yang and Y. Xie, *J. Am. Chem. Soc.* 131 (2009) 7218.
7. Y. Huang, X. F. Duan, Y. Cui, L. J. Lauhon, K. H. Kim and C. M. Lieber, *Science* 294 (2001) 1313.
8. M. S. Wu and H. H. Hsieh, *Electrochim. Acta* 53 (2008) 3427.
9. J. B. Goodenough and Y. Kim. *Chem. Mater.* 22 (2010) 587-603.
10. D. A. Notter, M. Gauch, R. Widmer, P. Wäger, A. Stamp, R. Zah and H.-J. Althaus. *Environ. Sci. Technol.* 44 (2010) 6550-6556.
11. B. Dunn, H. Kamath and J. M. Tarascon. *Science* 334 (2011) 928-935.
12. B. Scrosati, J. Hassoun and Y.-K. Sun. *Energy Environ. Sci.* 4 (2011) 3287-3295.
13. A. S. Aricò, P. Bruce, B. Scrosati, J.-M. Tarascon and W. Van Schalkwijk, *Nat. Mater.* 4 (2005) 366.
14. T. Ahmad, K. V. Ramanujachary, S.E. Lofland, A.K. Ganguli, *J. Mater. Chem.* 14 (2004) 3406–3410.
15. T. Ahmad, R. Chopra, K. V. Ramanujachary, S. E. Lofland and A. K. Ganguli, J. *Nanosci. Nanotechnol.* 5 (2005) 1840–1845.
16. T. Ahmad, S. Vaidya, N. Sarkar, S. Ghosh and A. K. Ganguli, *Nanotechnology* 17 (2006)1236–1240.
17. S. Vaidya, P. Rastogi, S. Agarwal, S. K. Gupta, T. Ahmad, A. M. Antonelli, K. V. Ramanujachary, S. E. Lofland and A. K. Ganguli, *J. Phys. Chem. C* 112 (2008)12610–12615.
18. J. Ahmed, T. Ahmad, K. V. Ramanujachary, S. E. Lofland and A. K. Ganguli, *J. Colloid Interface Sci*. 321 (2008) 434–441.
19. X. Zheng, G. H. He, X. C. Li and H. J. Liu, *Chem. Ind. Eng. Prog.* 26 (2007) 1159–1165.
20. M. Y. Li, W. S. Dong, C. L. Liu, Z. T. Liu and F. Q. Lin, *J. Cryst. Growth* 310 (2008) 4628–4634.
21. A. S. Khan, T. C. Devore and W. F. Reed, *J. Cryst. Growth* 35 (1976) 337–339.
22. W. W. Wang and Y. J. Zhu, *Mater. Res. Bull.* 40 (2005) 1929–1935.
23. X. R. Ye, D. Z. Jia, J. Q. Yu, X. Q. Xin and Z. L. Xue, *Adv. Mater.* 11 (1999) 941–942.
24. E. G. Gillan and R. B. Kaner, *Chem. Mater.* 8 (1996) 333–343.

25. W. Z. Wang, Y. J. Zhan and G. H.Wang, *Chem. Commun.* (2001) 727–728.
26. W. Z. Wang, Y. K. Liu, Y. J. Zhan and C. L. Zheng, *Mater. Res. Bull.* 36 (2001) 1977–1984.
27. F. Li, H. G. Zheng, D. Z. Jia, X. Q. Xin and Z. L. Xue, *Mater. Lett.* 53 (2002) 282–286.
28. Y. L. Cao, D. Z. Jia, L. Liu and J. M. Luo, *Chin. J. Chem.* 22 (2004) 1288–1290.
29. Z. P. Sun, L. Liu, L. Zhang and D. Z. Jia, *Nanotechnology* 17 (2006) 2266–2270.
30. L. Wang, B. Zhao, L. X. Chang and W. J. Zheng, *Sci. China Ser. B Chem.* 50 (2007) 224–229.
31. H. Pang, Y. Ma, G. Li, J. Chen, J. Zhang, H. Zheng and W. Du, *Dalton Trans.*, 41 (2012) 13284-13291.
32. H. Pang, Z. Yan, W. Wang, J. Chen, J. Zhang and H. Zheng, *Nanoscale*, 4 (2012) 5946-5953.
33. C. Z. Yuan, X. G. Zhang, L. H. Su, B. Gao, L. F. Shen, *J. Mater. Chem.*, 19 (2009) 5772–5777.
34. H. Pang, J. Deng, J. Du, S. Li, J. Li, Y. Ma, J. Zhang and J. Chen, *Dalton Trans.*, 41 (2012) 10175-10181.
35. H. Pang, Q. Y. Lu, C. Y. Chen, X. R. Liu and F. Gao, *J. Mater. Chem.*, 21 (2011) 13889-13894.
36. H. Pang, B. Zhang, J. M. Du, J. Chen, J. S. Zhang and S. J. Li, *RSC Adv.*, 2 (2012) 2257–2261.
37. M. Aragón, B. León, C. Vicente, and J. L. Tirado, *Inorg. Chem.* 47 (2008), 10366-10371.
38. W. W. Zhou, K. B. Tang, S. Y. Zeng and Y. X. Qi, *Nanotechnology* 19 (2008) 065602.
39. Y.Zhao , Y. Xie, S. Yan and X. Zhu, *Chem. Mater.* 20 (2008) 3959–3964
40. H. Pang,Z. Yan, Y. Ma, G. Li, J. Chen, J. Zhang, W. Du and S. Li, *J Solid State Electrochem* DOI 10.1007/s10008-013-2007-5
41. H. Pang, Z. Yan, Y. Wei, X. Li, J. Li, L. Zhang, J. Chen,J. Zhang and H. Zheng, *Part. Part. Syst. Charact.* 2013, acceptted.